Proceedings of the 7th International Conference of Control Systems, and Robotics (CDSR'20)
~~Niagara Falls, Canada~~ Virtual Conference – November, 2020
Paper No. 137
DOI: 10.11159/cdsr20.137

Position Control and Force Allocation Algorithms for Hybrid Pneumatic-Electric Linear Actuators

Behrad Rouzbeh, Gary M. Bone
Department of Mechanical Engineering/McMaster University
Hamilton, ON, Canada, L8S 4L7
rouzbehb@mcmaster.ca; gary@mcmaster.ca

Abstract **–** It has been shown that hybrid pneumatic electric actuators (HPEAs) can provide both accurate position control and high inherent safety, due to their low mechanical impedance; making them a suitable choice to be used in applications such as collaborative robots. HPEAs are redundant actuators that combine the large force, low bandwidth characteristics of pneumatic actuators with the large bandwidth, small force characteristics of electric actuators. If these characteristics are mathematically modelled, input allocation techniques can improve the HPEA performance by intelligently distributing the required input (force or torque) between the redundant actuators. In this study, after developing a model for a HPEA-driven system, a model-predictive control (MPC) approach is designed that employ this model and solve the position tracking and input allocation problem using convex optimization. Another approach based on conventional linear controllers is included and compared. Although the linear controller was more computationally-efficient, it was inferior to the MPC-based controller in position tracking and force allocation performance. The MPC-based controller with a two-layer structure reduced the position RMSE by 59%, the mean absolute electric actuator force by 36%, and the mean absolute pneumatic actuator force by 24% relative to the linear controller. It can also be computed fast enough for real-time operation.

Keywords**:** redundant actuators, hybrid pneumatic-electric actuators, force allocation, model predictive control, collaborative robots

1. Introduction

With recent growth in the field of collaborative robotics and their applications, enhancing robot safety has become an important area of research. Collaborative robots need to satisfy higher safety standards than conventional industrial robots [1]. Various approaches have been investigated for raising the level of safety in collaborative robots. They include active methods that monitor the environment and robot states using machine vision and/or sensor fusion and try to avoid risky situations; and passive methods that try to develop inherently safe robots that are not able to cause high damage in case of system failure or unpredicted situations. Using hybrid pneumatic-electric actuators (HPEA) in robots has been proposed as a solution to increase inherent safety without sacrificing precision [2][3].

Since the introduction of the HPEA idea in 1987 [4], different designs have been proposed to develop this type of actuator. They include a combination of a DC motor and a rotary pneumatic motor in parallel [5], pneumatic muscle actuators (PMA) with a DC motor [2][6][7], and pneumatic cylinders with a DC motor [8][9]. Recently the same concept has been used to develop a hybrid hydraulic-electric actuator for off-road vehicles [10].

With a hybrid actuator like HPEA, two actuators with different characteristics are performing the same task, which results in actuator redundancy. Since each of these actuators has completely distinct capabilities, HPEA's optimal performance can be obtained by systematically allocating the forces/torques between them according to their characteristics. Although there have been some papers focused on position controller design for HPEAs [6][9][3], very few have used a controller that incorporates each actuator's characteristics and studies allocation problem alongside the position control. In [7], an optimization method is proposed for the torque allocation of a HPEA consisting of a PMA and an electric motor. The performance of this method is limited since it uses only simplified actuator models.

In this paper, the position control and force allocation problem has been studied on a HPEA-driven system. The plant structure and its mathematical model have been presented. Then a model predictive controllers (MPC) has been designed and tested. MPC method is picked as it makes it possible to search for an optimal set of inputs in real-time that minimizes the designed objective function. This objective function can consider both tracking and input allocation criteria, as well as

the constraints of each actuator and the plant. The capability of this approach in real-time implementation has also been studied. As a comparison benchmark, another controller has been proposed using conventional linear controllers with no systematic input allocation strategy.

2. Plant Model

2.1. Plant Structure

The structure of the HPEA-driven system is shown in Fig. 1. A load mass is moving linearly on a horizontal low-friction surface. Two independent actuators are directly exerting force on this load in parallel. The first actuator is a pneumatic two-way cylinder with the two chambers defined by A and B; and the second one is a linear motor. To control the flow to/from each chamber, a three way proportional valve is used that operates with electric command signal. Two pressure controllers and a linear position sensor provide real-time feedback on the chamber pressures and the load position.

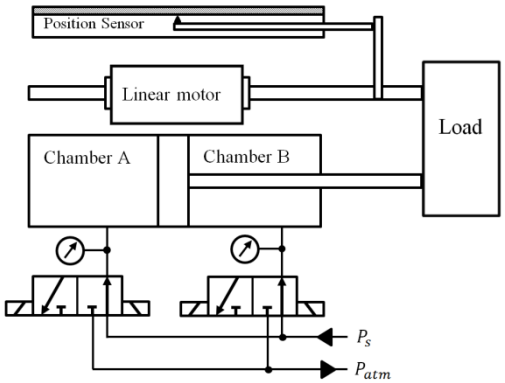

Fig. 1: Schematic illustration of the HPEA-driven system.

2.2. Mathematical Model

In this section mathematical equations are driven to model the system explained in 2.1. The dynamics of the load mass is defined by:

$$m_L \ddot{x}_p = F_p + F_e + F_f \tag{1}$$

where m_L, x_p, F_p, F_e, F_f are the load mass, load position, the force from the pneumatic cylinder, the electric motor's force, and the total friction force. The total friction force is modelled as viscous friction ($F_f = -C_v \dot{x}_p$).

It is known that the electric motor's response time is considerably smaller than the sampling time and the response times of other components. Thus, the motor's inner-dynamics can be neglected. If the relation between the motor force and the command signal to the motor is precisely known, we can consider F_e as an independent input to the position subsystem that can be provided accurately and instantaneously. The same assumptions cannot be made about the pneumatic force as it is a function of chamber pressures, which have significantly slower response time to the valve commands. In the next section the pneumatic force's dynamic model is derived.

The pneumatic force is the result of the difference in the forces at the two sides of the piston as indicated in (2). In this equation, P, A, and P_{atm} are the absolute chamber pressure, effective piston area of the chamber and the atmospheric pressure, respectively.

$$F_p = (P_A - P_{atm})A_A - (P_B - P_{atm})A_B \tag{2}$$

Deploying conservation of mass, conservation of energy and the ideal gas law for each chamber, leads to (3) and (4) [12]. In these equations $\dot{m}$, T, and R are the mass flow into the chamber, absolute temperature of the air, and

universal gas constant (287 Pa·m^3·K-1), respectively. L_A and L_B are the effective lengths of the chambers (considering the dead volumes) when the piston is at the origin.

$$\dot{P}_A = \frac{RT}{A_A(L_A + x_p)}\dot{m}_A - \frac{P_A}{L_A + x_p}\dot{x}_p \tag{3}$$

$$\dot{P}_B = \frac{RT}{A_B(L_B - x_p)}\dot{m}_B + \frac{P_B}{L_B - x_p}\dot{x}_p \tag{4}$$

In [11] the model for compressible flow through orifice area, and the ideal gas assumptions are used to develop a model for the mass flow rate through pneumatic valves. The mass flow is modelled as a function of the non-dimensional discharge coefficient of the valve (C_f), upstream and downstream pressures (P_u and P_d), and the valve orifice area (A_v) in choked and unchoked modes. For Enfield LS-V05s pneumatic valves, it has been shown [12] that the relation between the valve orifice area and the normalized spool displacement (z) can be approximated by fitting a curve in the form of (5), where $\lambda_1,\ldots,\lambda_7$ are the coefficients calculated using experimental data points and the least squares fitting method.

$$A_v = sign(z)\left(\lambda_1 + \lambda_2|z| + \lambda_3|z|^2 + \lambda_4|z|^3 + \lambda_5|z|^4\right)\left(1 - \tanh\left(\lambda_6|z| + \lambda_7\right)\right) \tag{5}$$

Regarding [12], the normalized spool displacement is related to the normalized command to the valve through a first-order transfer function with spool time constant of τ_v.

3. Controller Design

In this section two different controllers are designed to address the position control and input allocation tasks for the HPEA-driven system. The first controller is based on MPC to control position while the second one employs conventional linear controllers.

3.1. Two-Loop Controller with MPC

To simplify the optimization problem and make it computationally feasible, the coupling between the position sub-system and the pneumatic sub-system is neglected. In this approach only the position subsystem model is fed into the MPC and the valve models are not included in the optimization problem of MPC. This design requires a two-loop controller structure as the MPC block is responsible for controlling the position subsystem solely and independently. An inner-loop pressure controller handles the pneumatic subsystem and defines the command signals to each valve. The schematic of this control system structure is illustrated in Fig. 2.

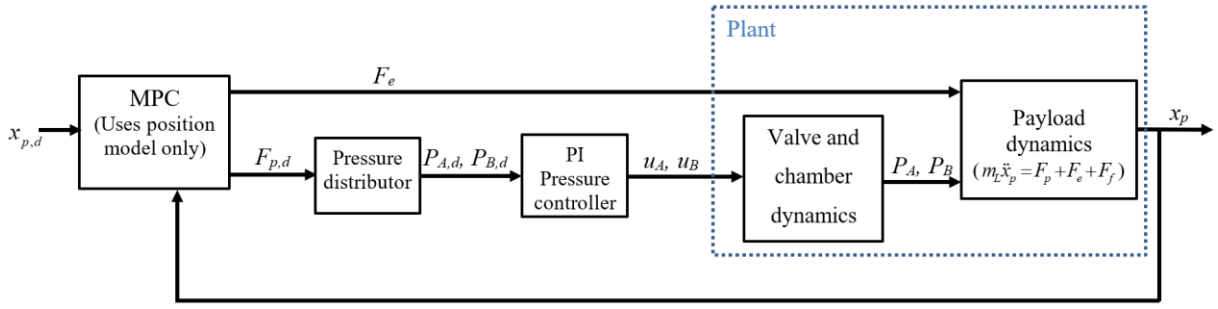

Fig. 2: Controller structure with MPC

The MPC block uses (2) to derive linear state space model in the format shown in (6). The subscripts (k and k+1) denote the sample counter.

$$\mathbf{x}(k+1)=\mathbf{A}\mathbf{x}(k)+\mathbf{B}\mathbf{u}(k) \quad , \quad \mathbf{y}(k)=\mathbf{C}\mathbf{x}(k)+\mathbf{D}\mathbf{u}(k) \tag{6}$$

The states, inputs and output are as follows.

$$\mathbf{x}(k)=\begin{bmatrix} x_{p(k)} & \dot{x}_{p(k)} \end{bmatrix}^T \quad , \quad \mathbf{u}(k)=\begin{bmatrix} F_{p,d(k)} & F_{e(k)} \end{bmatrix}^T \quad , \quad \mathbf{y}(k)=x_{p(k)} \tag{7}$$

The MPC continuously solves the optimization problem (8) every sampling instant with a prediction horizon of N_p points, by using a time-efficient convex optimization algorithm. Here **R** is the reference input (desired position), and **Q**, $\mathbf{R_1}$ and $\mathbf{R_2}$ are positive-definite gain matrices. The last constraint in (8) limits the changes in $\boldsymbol{U}$ between two consecutive samples, as the MPC has no sense of the inner dynamics of the pressure subsystems and its limitations.

$$\begin{aligned}
&\underset{\mathbf{u}}{\textit{minimize}} \quad \sum_{i=1}^{N_p}((\mathbf{y}(k+i)-\mathbf{r}(k+i))^T\mathbf{Q}(\mathbf{y}(k+i)-\mathbf{r}(k+i))... \\
&\qquad +(\mathbf{u}(k+i))^T\mathbf{R}_1\mathbf{u}(k+i)+(\mathbf{u}(k+i)-\mathbf{u}(k+i-1))^T\mathbf{R}_2(\boldsymbol{u}(k+i)-\mathbf{u}(k+i-1)) \\
&\textit{subject to} \\
&\qquad \mathbf{x}(k+j+1)=\mathbf{A}\mathbf{x}(k+j)+\mathbf{B}\mathbf{u}(k+j) \quad , j=0,...,N_p-1 \\
&\qquad \mathbf{y}(k+j)=\mathbf{C}\mathbf{x}(k+j)+\mathbf{D}\mathbf{u}(k+j) \quad , j=1,...,N_p \\
&\qquad \mathbf{u}_{\min}\le\mathbf{u}(k+j)\le\mathbf{u}_{\max} \quad , j=1,...,N_p \\
&\qquad \mathbf{x}_{\min}\le\boldsymbol{x}(k+j)\le\mathbf{x}_{\max} \quad , j=1,...,N_p \\
&\qquad \Delta\mathbf{u}_{\min}\le\mathbf{u}(k+j)-\mathbf{u}(k+j-1)\le\Delta\mathbf{u}_{\max} \quad , j=1,...,N_p
\end{aligned} \tag{8}$$

Before feeding $F_{p,d}$ from the outer-loop position controller to the inner-loop pressure controller, the pressure distributor should define the desired chamber pressures. This is done by satisfying the two conditions $(P_{A,d}(k)-P_{atm})A_A-(P_{B,d}(k)-P_{atm})A_B=F_{p,d}(k)$, and $\left(P_{A,d}(k)+P_{B,d}(k)\right)/2=P_{mid}$ where $P_{mid}=\left(P_s+P_{atm}\right)/2$. The solution to these conditions is shown in (9).

$$P_{A,d(k)}=\frac{2P_{mid}+\left(\frac{A_A}{A_B}-1\right)P_{atm}+\frac{F_{p,d(k)}}{A_B}}{\frac{A_A}{A_B}+1} \quad , \quad P_{B,d(k)}=\frac{2P_{mid}+\left(\frac{A_B}{A_A}-1\right)P_{atm}-\frac{F_{p,d(k)}}{A_A}}{\frac{A_B}{A_A}+1} \tag{9}$$

A conventional PI controller, with bounded integral term, is used to control chamber pressures as shown in (10). Here, t(k) denotes time at the kth sample.

$$u_j(k)=K_{p,p}\left(P_{j,d}(k)-P_j(k)\right)+K_{I,p}\int_0^{t(k)}\left(P_{j,d}(k)-P_j(k)\right)dt \quad , j\in\{A,B\} \tag{10}$$

3.2. Linear Two-Loop Controller

As a comparison benchmark, a conventional linear position controller is also designed and tested. The controller structure is the same as that of Fig. 2, except for replacing the MPC block with a linear position controller. This controller structure is similar to the two-loop structure used in [3]. Two independent controllers are used with the pneumatic and the electric actuators, with the former using feedforward + PD controller and the latter using PD

controller. The feedforward term compensates for inertial and friction loads. The equations for these controllers are shown in (11) and (12).

$$F_{p,d}(k) = m_L \ddot{x}_{p,d}(k) + \hat{C}_v \dot{x}_p(k) + K_{P,c}\left(x_{p,d}(k) - x_p(k)\right) + K_{D,c}\left(\dot{x}_{p,d}(k) - \dot{x}_p(k)\right) \tag{11}$$

$$F_e(k) = K_{P,m}\left(x_{p,d}(k) - x_p(k)\right) + K_{D,m}\left(\dot{x}_{p,d}(k) - \dot{x}_p(k)\right) \tag{12}$$

5. Results and discussion

The two controllers are simulated and compared using MATLAB running on a Windows 10 PC with an Intel Core i5 processor. To challenge the tracking and force allocation performance, a relatively large payload mass of $m_L = 10\,\text{kg}$ is used. The pneumatic actuator parameters are adopted from a SMC NCMB106 air cylinder [3] and a Enfield LS-V05s pneumatic valve [12]. An uncertainty of 20% has been included in the friction coefficient $\hat{C}_v$ (i.e. $\hat{C}_v = 0.8C_v$). The plant and controller parameters are listed in Table 1. Fig. 3 shows the results from each controller. They follow a reference trajectory made up of step inputs and a slower 1Hz sine wave then a faster 4Hz sine wave. For easier comparison, the tracking errors are plotted on the same axes in Fig. 4.

Table 1: Plant and controller parameters.

Parameter	Value	Parameter	Value
A_A	5.720×10^{-4} m^2	P_{atm}	101000 Pa
A_B	5.227×10^{-4} m^2	P_s	404000 Pa
C_f	0.5393	$\mathbf{Q}$	10^6
C_v	44.4 Ns/m	$\mathbf{R}_2$	diag([0.1,0])
$\hat{C}_v$	35.5 Ns/m	$\Delta\mathbf{u}_{\min}$	$[-30,-60]^T$
$K_{P,c}$	2000 N/m	$\Delta\mathbf{u}_{\max}$	$[30, 60]^T$
$K_{D,c}$	30 Ns/m	λ_1	0.585
$K_{P,m}$	500 N/m	λ_2	-7.51
$K_{D,m}$	50 Ns/m	λ_3	38.1
$K_{p,p}$	5×10^{-5} Pa^{-1}	λ_4	-46.9
$K_{I,p}$	5×10^{-4} Pa^{-1}s^{-1}	λ_5	18.2
L_A	0.1316 m	λ_6	-21.3
L_B	0.1316 m	λ_7	3.42
m_L	10 kg	τ_v	0.0015 s

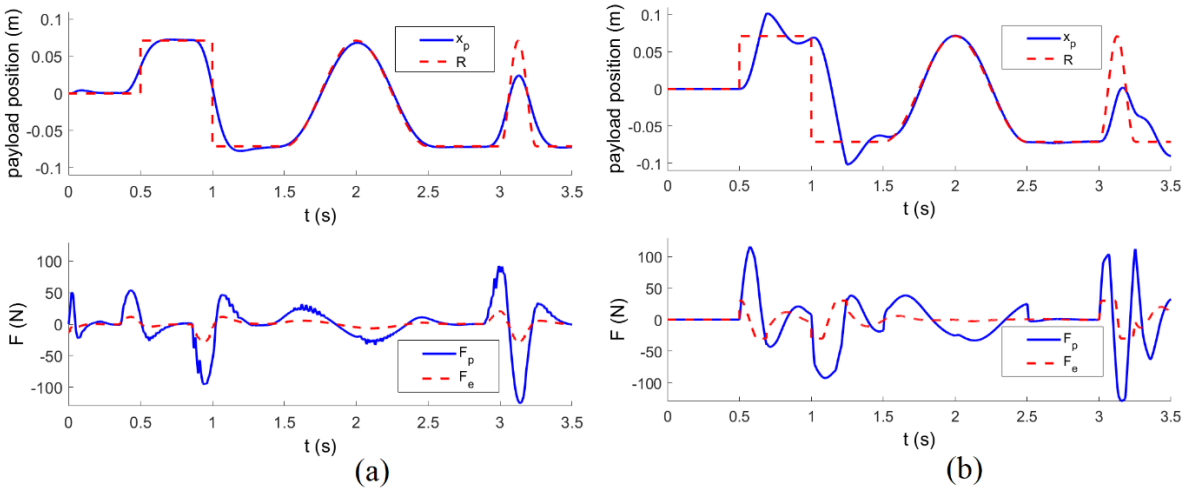

Fig. 3: Position tracking and force allocation performance using: (a) MPC, (b) linear controller.

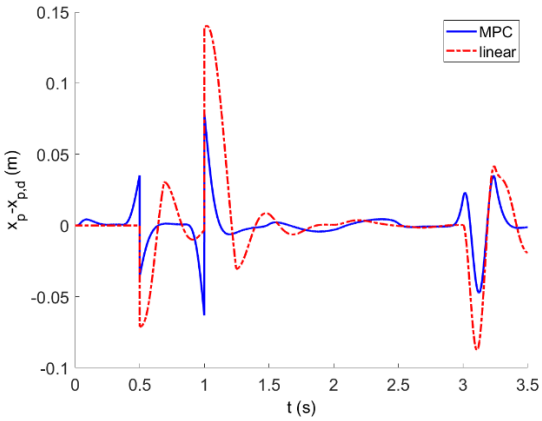

Fig. 4: Comparison of the position tracking errors with the two controller approaches

It can be seen that the linear controller has longer settling time, and significantly larger error peaks when subjected to the faster trajectories of 4 Hz and above. The MPC controller demonstrates smoother and more accurate results. A quantitative comparison is presented in Table 2. Although the linear controller has the lower accuracy, it has a much faster calculation time. The MPC yields the best tracking performance with RMSE reduction of 59% compared to the linear controller. This controller also reduced the mean absolute electric actuator force by 36%, and the mean absolute pneumatic actuator force by 24% relative to the linear controller.

6. Conclusion

In this paper, two control algorithms for the position control of HPEA are investigated. The first one uses an outer-loop MPC with a PI with bounded integral term inner-loop pressure controller, and the second one uses an outer-loop PD plus feedforward controller with the same inner-loop pressure controller. The MPC-based approach demonstrated superior position tracking and force allocation performance. It reduced the position RMSE by 59%, the mean absolute pneumatic actuator force by 24% and the mean absolute electric actuator force by 36%. The force reduction has the benefit of reducing the energy consumed by the actuator. Although the MPC-based approach is computationally intensive, it can still be run in real-time using commonly available hardware.

Table 2: Numerical comparison of the controllers

Parameter	Value	
	MPC	Linear
Prediction horizon (N_p)	15	-
Sampling time (T_s)	10 ms	1 ms
Simulation integration time	0.5 ms	0.5 ms
Position tracking RMSE	13.1 mm	31.9 mm
Mean Absolute F_p	19.83 N	26.11 N
Mean Absolute F_e	4.73 N	7.41 N
Average calculation time per sample	7.48 ms	0.006 ms

Acknowledgements

The funding provided by the Natural Sciences and Engineering Research Council of Canada (NSERC) through a Discovery Grant is gratefully acknowledged.

References

[1] ISO/TS 15066:2016, Robots and robotic devices - Collaborative robots. International organization for standardization, 2016.

[2] D. Shin, I. Sardellitti, and O. Khatib, “A hybrid actuation approach for human-friendly robot design,” in: Proc. IEEE Int. Conf. Robot. Autom., 2008, pp. 1747–1752.

[3] B. Rouzbeh, G. M. Bone, G. Ashby, and E. Li, “Design, Implementation and Control of an Improved Hybrid Pneumatic-Electric Actuator for Robot Arms,” IEEE Access, vol. 7, pp. 14699–14713, 2019.

[4] L. J. Petrosky, “Hybrid electro-pneumatic robot joint actuator,” U.S. Patent 478 225 828, October 1987.

[5] F. Takemura, S. Pandian, Y. Nagase, H. Mizutani, Y. Hayakawa, and S. Kawamura, “Control of a hybrid pneumatic/electric motor,” in Proc. IEEE/RSJ Int. Conf. Intelligent Robots and Syst., 2000, pp. 209–214.

[6] T. Teramae, T. Noda, Sang-Ho Hyon, and J. Morimoto, “Modeling and control of a Pneumatic-Electric hybrid system,” in 2013 IEEE/RSJ Int. Conf. Intelligent Robots and Systems, 2013, vol. 4, no. 8, pp. 4887–4892.

[7] K. Ishihara and J. Morimoto, “An optimal control strategy for hybrid actuator systems: Application to an artificial muscle with electric motor assist,” Neural Networks, vol. 99, pp. 92-100, 2018.

[8] G. M. Bone and X. Chen, “Position control of hybrid pneumatic-electric actuators,” in Proc. American Control Conf., 2012, pp. 1793–1799.

[9] G. M. Bone, M. T. Xue and J. Flett, "Position control of hybrid pneumatic–electric actuators using discrete-valued model-predictive control", Mechatronics, vol. 25, pp. 1–10, 2015.

[10] P. Y. Li, J. Siefert, and D. Bigelow, “A Hybrid Hydraulic-Electric Architecture (HHEA) for High Power Off-Road Mobile Machines,” in ASME/BATH 2019 Symposium on Fluid Power and Motion Control, 2019.

[11] E. Richer and Y. Hurmuzlu, “A high performance pneumatic force actuator system: Part I—nonlinear mathematical model,” *J. Dyn. Syst. Meas. Control. Trans. ASME*, vol. 122, no. 3, pp. 416–425, 2000.

[12] B. Taheri, D. Case, and E. Richer, “Force and stiffness backstepping-sliding mode controller for pneumatic cylinders,” IEEE/ASME Trans. Mechatronics, vol. 19, no. 6, pp. 1799–1809, 2014.